Understanding the X-ray spectrum of anomalous X-ray pulsars and soft gamma-ray repeaters

2015 Res. Astron. Astrophys. 15 525

(http://iopscience.iop.org/1674-4527/15/4/525)

RAA 2015 Vol. **15** No. **4**, 525–536 doi: 10.1088/1674–4527/15/4/006
http://www.raa-journal.org *http://www.iop.org/journals/raa*

Research in Astronomy and Astrophysics

Understanding the X-ray spectrum of anomalous X-ray pulsars and soft gamma-ray repeaters *

Yan-Jun Guo[1], Shi Dai[1], Zhao-Sheng Li[1], Yuan Liu[2], Hao Tong[3] and Ren-Xin Xu[1,4]

[1] School of Physics and State Key Laboratory of Nuclear Physics and Technology, Peking University, Beijing 100871, China; *guoyj10@pku.edu.cn*
[2] Institute of High Energy Physics, Chinese Academy of Sciences, Beijing 100049, China
[3] Xinjiang Astronomical Observatory, Chinese Academy of Sciences, Urumqi 830011, China
[4] Kavli Institute for Astronomy and Astrophysics, Peking University, Beijing 100871, China

Received 2014 March 26; accepted 2014 July 14

Abstract Hard X-rays above 10 keV are detected from several anomalous X-ray pulsars (AXPs) and soft gamma-ray repeaters (SGRs), and different models have been proposed to explain the physical origin within the frame of either a magnetar model or a fallback disk system. Using data from *Suzaku* and INTEGRAL, we study the soft and hard X-ray spectra of four AXPs/SGRs: 1RXS J170849–400910, 1E 1547.0–5408, SGR 1806–20 and SGR 0501+4516. It is found that the spectra could be well reproduced by the bulk-motion Comptonization (BMC) process as was first suggested by Trümper et al., showing that the accretion scenario could be compatible with X-ray emission from AXPs/SGRs. Simulated results from the Hard X-ray Modulation Telescope using the BMC model show that the spectra would have discrepancies from the power-law, especially the cutoff at $\sim$200 keV. Thus future observations will allow researchers to distinguish different models of the hard X-ray emission and will help us understand the nature of AXPs/SGRs.

Key words: stars: neutron — pulsars: individual (1E 1547.0–5408, 1RXS J170849–400910, SGR 0501+4516, SGR 1806–20) — X-rays: stars

1 INTRODUCTION

Since the discovery of radio pulsars in 1967, various kinds of pulsar-like objects have been observed, which exhibit diverse manifestations. Among them, anomalous X-ray pulsars (AXPs) and soft gamma-ray repeaters (SGRs) are peculiar kinds of sources (Mereghetti 2008). Their persistent X-ray luminosities are much higher than spin down energy, but no binary signature has been observed, thus ruling out both rotation and accretion in a binary system as the power source. They also show recurrent bursts in the hard X-ray/soft gamma-ray band and even giant flares, which could be highly super-Eddington. In addition, AXPs/SGRs have long spin periods clustered in the range of 2–12 s, and their period derivatives are also large.

Conventional models for AXPs/SGRs are magnetars (Duncan & Thompson 1992), isolated neutron stars with extremely strong dipole and multipole magnetic fields (higher than the quantum

* Supported by the National Natural Science Foundation of China.

critical magnetic field $B_{\rm QED} = m_e^2 c^3/e\hbar = 4.4 \times 10^{13}$ G). The persistent emission is powered by magnetic field decay; magnetic dipole radiation would contribute to their spin-down, and the effects of a twisted magnetosphere (Thompson et al. 2002) and wind braking (Tong et al. 2013) have also been considered. A sudden release of magnetic energy, such as magnetic reconnection, could result in bursts or giant flares. Although the magnetar model could explain some of the properties of AXPs/SGRs, it is still facing some problems arising from accumulating observations: few predictions have been confirmed yet. After all, there is no direct evidence for the existence of a super-strong magnetic field. Alternative models of AXPs/SGRs are not only possible but also welcome.

AXPs/SGRs are suggested to be pulsar-like objects with a normal field accreting from supernova fallback disks (Chatterjee et al. 2000; Alpar 2001). Accretion energy could power the persistent emission, and the propeller effect may account for the braking mechanism, as well as the period clustering of AXPs/SGRs. However, fallback disk models could not explain the super-Eddington bursts or giant flares. The problem could be solved if the compact star is a solid quark star (Xu 2003), since the self-confined surface (Alcock et al. 1986) could explain the super-Eddington phenomena, and the energy released during star quakes (Xu et al. 2006) may be an alternative power source for bursts and giant flares. Therefore, AXPs/SGRs could be quark star/fallback disk systems (Xu 2007; Tong & Xu 2011).

Determining whether AXPs/SGRs are magnetars or fallback disk systems is of fundamental importance. It could help us understand the observational phenomena of AXPs/SGRs, and even give hints on the nature of pulsar-like stars, which is related to the state of cold matter at supranuclear density where strong interactions play an important role. In this paper, we would like to study the problem from the perspective of the X-ray spectrum of AXPs/SGRs. AXPs/SGRs have soft spectra below 10 keV that are generally fitted by a combination of a steep power-law with photon index $\Gamma \sim 2-4$ and a blackbody with temperature $kT \sim 0.5$ keV (Mereghetti 2008). Non-thermal hard X-ray components above 15 keV in AXPs/SGRs were discovered in recent years, with different spectral properties from the soft X-ray band (Kuiper et al. 2006). The hard X-ray spectra are well fitted by flat power-laws with photon index $\Gamma \sim 0.5-1.5$, and the luminosity is similar to that of the soft X-ray band. Therefore, the hard X-rays provide us with important information to understand the magnetic fields and surface properties, and could put strong constraints on the theoretical modeling of AXPs/SGRs. The physical mechanism of hard X-ray emission is still unknown, but some possibilities have been proposed that try to explain it.

In the frame of magnetars, a quantum electrodynamics model (Heyl & Hernquist 2005), bremsstrahlung model (Beloborodov & Thompson 2007) and resonant inverse Compton scattering model (Baring & Harding 2007) have been explored, predicting power-law spectra with different cutoff properties. The spectral cutoff properties of AXPs/SGRs are not well understood yet. Upper limits in MeV bands are obtained with the archival CGRO COMPTEL data of four AXPs, which indicate cutoff energy is below 1 MeV (Kuiper et al. 2006). 4U 0142+61 is the brightest AXP. The time-averaged spectra of 4U 0142+61, extracted from INTEGRAL IBIS data that have accumulated over nine years, can be fitted using a power-law with an exponential cutoff at ~ 130 keV. This aspect might rule out models involving ultrarelativistic electrons (Wang et al. 2013). In the context of a fallback disk, Trümper et al. (2010) considered producing the hard X-ray emission by the bulk-motion Comptonization (BMC) process of surface photons in the accretion flow. Their work shows that for 4U 0142+61, the BMC model could reproduce both the soft and hard X-ray spectra. The BMC model is successful in explaining the spectra of 4U 0142+61, but its applicability to other sources remains in doubt.

In this work, we study the broadband X-ray spectrum of AXPs/SGRs, try to put further constraints on the BMC model, and perform a simulation to discuss how to distinguish different models by future observations. Using data from *Suzaku* and the INTErnational Gamma-Ray Astrophysics Laboratory (INTEGRAL), we derive the soft and hard X-ray spectra of four sources, namely AXP 1RXS J170849–400910, AXP 1E 1547.0–5408, SGR 1806–20 and SGR 0501+4516 (hereafter ab-

breviated 1RXS J1708–40, 1E 1547–54, SGR 1806–20 and SGR 0501+45, respectively). We find that the spectra of all the chosen sources can be well fitted with the XSPEC model compTB, showing that the accretion scenario could be compatible with X-ray emission from AXPs/SGRs. To investigate the feasibility of discriminating various models of hard X-ray emission by future observations, we also simulate results from the Hard X-ray Modulation Telescope (HXMT)[1]. Simulated spectra from the BMC model exhibit a cutoff around 200 keV, which could distinguish BMC from other cases in the magnetar model.

In Section 2 we will introduce the *Suzaku* and INTEGRAL observations that we utilized, along with data analysis including spectral properties and time variabilities. Then we present the averaged spectra and the fitting of the compTB model in Section 3. HXMT simulations are shown in Section 4, and possible discrepancies between various models of the hard X-ray emission are also discussed. Finally we draw our conclusions in Section 5.

2 OBSERVATIONS AND DATA ANALYSIS

2.1 Source Selection

Suzaku provides simultaneously observed soft and hard X-ray spectra from seven AXPs/SGRs (Enoto et al. 2010a) for the first time. Among these seven sources, SGR 1900+14 is only detected up to $\sim$50 keV due to its relatively low flux, and the soft X-ray spectrum of 1E 1841–045 is contaminated by emission lines from the surrounding supernova remnant (see Enoto et al. 2010a, fig. 1). Therefore, in our analysis we will only focus on four sources, namely 1RXS J1708–40, 1E 1547–54, SGR 1806–20 and SGR 0501+45; the data from 4U 0142+61, SGR 1900+14 and 1E 1841–045 are not analyzed. For the hard X-ray spectra, INTEGRAL observations are also used, which could reach higher energy and place better constraints on parameters. Because the hard X-ray detector on INTEGRAL has a lower sensitivity than the detector on *Suzaku*, the spectrum from a single observation has to be summed up to get an acceptable signal-to-noise ratio (S/N). The spectral fitting software used is XSPEC version 12.8.0, and all cited errors are at the 1σ level.

2.2 *Suzaku* Observations

Suzaku observations utilized to extract spectra of the four sources are listed in Table 1. We extracted spectra using data from the X-ray Imaging Spectrometer (XIS; Koyama et al. 2007) and the Hard X-ray Detector (HXD; Takahashi et al. 2007), which are sensitive in the energy range of 0.2–12 keV and 10–70 keV respectively. The data reduction was carried out using HEASOFT version 6.13. The XIS and HXD data were reprocessed with the pipeline processing version 2.4, employing the recommended data screening criteria. We accumulated screened data of XIS from a region within a $2'$ radius of the source centroid, and derived a background spectrum from source-free regions in the immediate vicinity of the target. For HXD-PIN data, non-X-ray background and cosmic X-ray background were subtracted to obtain spectra.

We fit the soft X-ray spectra with a two component blackbody plus power-law model affected by photoelectric absorption, and the hard X-ray spectra with a single power-law model. The fitting results, as shown in Table 2, of 1RXS J1708–40 and SGR 1806–20 are in agreement with values from other observations of the sources within error (Rea et al. 2007; Esposito et al. 2007; Enoto et al. 2010a). Since 1E 1547–54 and SGR 0501+45 are in outburst during the *Suzaku* observations we used, it is not feasible to compare the fitting parameters with observations in quiescent states. So, we fit the broadband spectra of 1E 1547–54 with a two component blackbody plus a power-law model, while a three component model including two blackbodies and a power-law is applied to SGR 0501+45, as tried in a previous analysis of the same observations (Enoto et al. 2010b,c), and

[1] *http://heat.tsinghua.edu.cn/hxmtsci/hxmt.html*

Table 1 *Suzaku* and INTEGRAL Observations

Name	*Suzaku* ObsID	Time span (yy/mm/dd)	Exposure (ks)	INTEGRAL Revs.	Time span (yy/mm/dd)	Exposure (Ms)
1RXS J1708–40	404080010	09/08/23 – 09/08/24	47.9	0037 – 1088	03/02/01 – 11/09/13	5.84
1E 1547–54	903006010	09/01/28 – 09/01/29	31.0	0767 – 0769	09/01/28 – 09/02/01	0.16
SGR 1806–20	402094010	07/10/14 – 07/10/15	46.6	0286 – 1080	05/02/16 – 11/08/20	4.24
SGR 0501+45	903002010	08/08/26 – 08/08/27	50.7	0047 – 1141	03/03/03 – 12/02/17	1.45

Notes: The observation time and exposure of INTEGRAL are for the data selected to derive time-averaged spectra, which could be different from those of all the available observations.

Table 2 Soft and Hard X-ray Spectral Properties of *Suzaku* Data

Name	Model[a]	$N_{\rm H}$ (10^{22} cm^{-2})	kT (keV)	Γ	χ^2/d.o.f.	Flux[b] soft/hard
1RXS J1708–40	BB+PL	1.40 ± 0.04	0.45 ± 0.01	2.72 ± 0.07	1.23 (169)	3.17 ± 0.01 / –
1E 1547–54	BB+PL	$3.46^{+0.21}_{-0.22}$	$0.61^{+0.04}_{-0.03}$	$2.38^{+0.19}_{-0.22}$	1.01 (87)	6.63 ± 0.07 / –
SGR 1806–20	BB+PL	$8.43^{+1.07}_{-0.96}$	$0.40^{+0.09}_{-0.06}$	$1.97^{+0.17}_{-0.20}$	1.09 (80)	0.95 ± 0.02 / –
SGR 0501+45	BB+PL	1.06 ± 0.02	0.69 ± 0.01	2.96 ± 0.04	1.11 (231)	2.94 ± 0.01 / –
1RXS J1708–40	PL	–	–	1.73 ± 0.18	0.94 (9)	– / 2.59 ± 0.33
1E 1547–54	PL	–	–	1.55 ± 0.08	1.05 (16)	– / 9.34 ± 0.05
SGR 1806–20	PL	–	–	1.69 ± 0.15	0.94 (16)	– / 2.98 ± 0.32
SGR 0501+45	PL	–	–	0.43 ± 0.26	0.99 (7)	– / 3.05 ± 0.45
1RXS J1708–40	2BB+PL	$1.24^{+0.06}_{-0.05}$	$0.33\pm0.03/0.64\pm0.04$	1.59 ± 0.07	1.16 (178)	3.11 ± 0.02 / 2.74 ± 0.21
1E 1547–54	BB+PL	2.81 ± 0.08	0.65 ± 0.02	1.54 ± 0.05	1.10 (105)	6.83 ± 0.05 / 9.39 ± 0.04
SGR 1806–20	BB+PL	$6.40^{+0.58}_{-0.50}$	$0.61^{+0.07}_{-0.06}$	$1.32^{+0.05}_{-0.06}$	0.98 (94)	1.12 ± 0.02 / 3.64 ± 0.21
SGR 0501+45	2BB+PL	0.73 ± 0.03	$0.33\pm0.02/0.73\pm0.01$	$1.35^{+0.12}_{-0.11}$	1.13 (238)	2.95 ± 0.01 / 1.90 ± 0.19

Notes: The first four rows are BB+PL fitting to the soft X-ray spectra; the middle four rows are PL fitting to the hard X-ray spectra; the last four rows are fitting results of broadband X-ray spectra.

[a] BB and PL represent blackbody and power-law respectively.

[b] 2–10 keV flux for soft spectra and 20–60 keV flux for hard spectra, in units of 10^{-11} erg cm^{-2} s^{-1}.

the parameters are also consistent with former results. The spectral properties during the outburst are similar to those of the source in quiescence.

2.3 INTEGRAL Observations

The gamma-ray mission INTEGRAL (Winkler et al. 2003) has been operational since October 2002. Its imager IBIS (Imager on Board the INTEGRAL Satellite; Ubertini et al. 2003) has a low-energy detector sensitive between 20–300 keV, named the INTEGRAL Soft Gamma-Ray Imager (ISGRI; Lebrun et al. 2003). We used all public data from the INTEGRAL Science Data Center (ISDC) where the sources are within 10° of the pointing direction from 2003 to 2011. The IBIS-ISGRI data were reduced with the Off-line Scientific Analysis (OSA) software version 10. Following the standard procedures described in the IBIS analysis user manual, we created images in four energy bands (20–40, 40–60, 80–100, 100–300 keV) for source detection and extracted spectra of the sources for each individual pointing.

To get a better S/N, spectra of individual pointings are summed up to derive the time-averaged spectra. Even so, the significance level of detection for SGR 0501+45 is very low (2.72σ), making it impossible to extract a spectrum with high S/N, so we only analyze INTEGRAL spectra of the other three sources. Considering possible variability of the sources over such a long time, we divide the INTEGRAL observations from 2003 to 2011 into one-year time intervals and extract spectra

Table 3 Time Variations of INTEGRAL Observations

	1RXS J1708–40			1E 1547–54			SGR 1806–20		
Year	Γ	Flux[a]	χ^2/d.o.f.	Γ	Flux[a]	χ^2/d.o.f.	Γ	Flux[a]	χ^2/d.o.f.
2003	$0.79^{+0.28}_{-0.29}$	3.82±0.64	1.25 (9)	1.24±2.26	$0.43^{+1.74}_{-0.35}$	1.71 (9)	1.70±0.10	$6.83^{+0.23}_{-0.22}$	0.87 (9)
2004	$1.40^{+0.46}_{-0.42}$	$3.48^{+0.89}_{-0.88}$	0.60 (9)	$0.81^{+0.60}_{-0.63}$	1.16±0.49	0.91 (9)	1.77±0.06	12.0±0.2	1.72 (9)
2005	0.67±0.24	3.10±0.52	1.10 (9)	0.58±1.09	$0.61^{+0.65}_{-0.66}$	1.64 (9)	1.56±0.14	$5.73^{+0.31}_{-0.30}$	0.74 (9)
2006	$0.91^{+0.34}_{-0.36}$	4.22±0.87	1.21 (9)	–	–	–	1.36 ±0.13	6.57±0.33	0.87 (9)
2007	$1.05^{+0.34}_{-0.36}$	$3.10^{+0.80}_{-0.79}$	1.10 (9)	$0.67^{+0.46}_{-0.49}$	4.71±1.76	1.25 (9)	$1.84^{+0.25}_{-0.23}$	$3.90^{+0.31}_{-0.30}$	0.58 (9)
2008	$0.71^{+0.51}_{-0.49}$	5.47±1.83	0.70 (9)	0.85±1.77	$1.73^{+3.01}_{-1.10}$	1.96 (9)	$1.78^{+0.59}_{-0.48}$	$4.65^{0.68}_{-0.67}$	1.69 (9)
2009	$1.26^{+0.39}_{-0.37}$	$5.70^{+1.33}_{-1.31}$	1.13 (9)	1.39±0.06	18.0±0.7	0.83 (9)	$1.52^{+0.54}_{-0.44}$	$4.95^{+0.78}_{-0.79}$	1.09 (9)
2010	$1.28^{+0.21}_{-0.20}$	4.34 ±0.56	1.23 (9)	0.74±0.17	9.29±0.99	0.75 (9)	$1.36^{+0.34}_{-0.33}$	$5.23^{+0.64}_{-0.63}$	0.92 (9)
2011	0.84±0.28	$4.16^{+0.83}_{-0.84}$	1.49 (9)	–	–	–	$1.25^{+0.35}_{-0.33}$	6.42±0.71	1.15 (9)
average	0.95±0.12	4.01±0.23	1.82 (6)	1.57±0.09	21.0±1.3	1.07 (8)	1.49±0.08	5.46±0.29	1.44 (8)

Notes: [a] 20–150 keV flux in units of 10^{-11} erg cm^{-2} s^{-1}.

respectively. The spectra are fitted with a single power-law model, and the fitting results as well as 20–150 keV fluxes are listed in Table 3. We also plot the photon indices Γ and fluxes in Figure 1.

For 1RXS J1708–40, the deviation of photon indices and fluxes from the time averaged value is within the 2σ level, thus there is no significant variation. In the case of SGR 1806–20, the fluxes in 2003 and 2004 are apparently higher than those of the other years, presumably due to its giant flare in 2004 (Hurley et al. 2005). In the following seven years, the fluxes and photon indices do not change significantly, so we only sum up spectra of observations from 2005 to 2011.

However, the fluxes of 1E 1547–54 vary dramatically and an outburst is observed in 2009, during which its hard X-ray emission was first discovered by *Suzaku*. For compatibility with *Suzaku* soft X-ray data of 1E 1547–54, the INTEGRAL observations utilized are only Revs. 768–769, from 2009 January 28 to 2009 February 1, which overlap in time with *Suzaku* observations from 2009 January 28 to 2009 January 29. As both the soft and hard spectra vary slightly from 2009 January 28 to 2009 February 7 (Bernardini et al. 2011), the longer time span of INTEGRAL observations than that of *Suzaku* observations would make little difference.

The selection of INTEGRAL data for the three sources to get averaged spectra is analyzed above, and we summarize the resulting total exposure time in Table 1. We also fit the averaged spectra with a power-law model, and the fitting results are given in Table 3.

3 APPLICATION OF BMC MODEL TO THE AVERAGED SPECTRA

If AXPs/SGRs are fallback disk systems, soft photons emitted from the polar cap would be in the accretion flow. Some of the seed photons get upscattered by the Comptonization process with high-energy electrons, producing the hard X-ray emission, while others escape directly and constitute the soft X-ray spectra (Trümper et al. 2010). In spectral fitting, the BMC process is described by the XSPEC model compTB (Farinelli et al. 2008), in which thermal and bulk-motion Comptonization of seed photons are considered. This model consists of two components, the direct seed photon spectrum and the Comptonized spectrum obtained as a self-consistent convolution of the seed spectrum with the system's Green function. The seed photon spectrum is a modified blackbody $S(E) \propto E^{\gamma}/(e^{E/kT_{\rm s}}-1)$, where $kT_{\rm s}$ is the blackbody temperature and γ represents a modification of the blackbody. The Comptonization process is characterized by three parameters, bulk parameter $\delta = \langle E_{\rm bulk}\rangle/\langle E_{\rm th}\rangle$ describing the relative efficiency of bulk over thermal Comptonization, electron temperature $kT_{\rm e}$ and energy index of the Comptonization spectrum α. There are also two coefficients, illumination factor A and normalization of the seed photon spectrum $C_{\rm N}$.

First we fit the broadband *Suzaku* spectra of the four sources with compTB, which provides good fits from a statistical point of view. However, when initial values of parameters are changed,

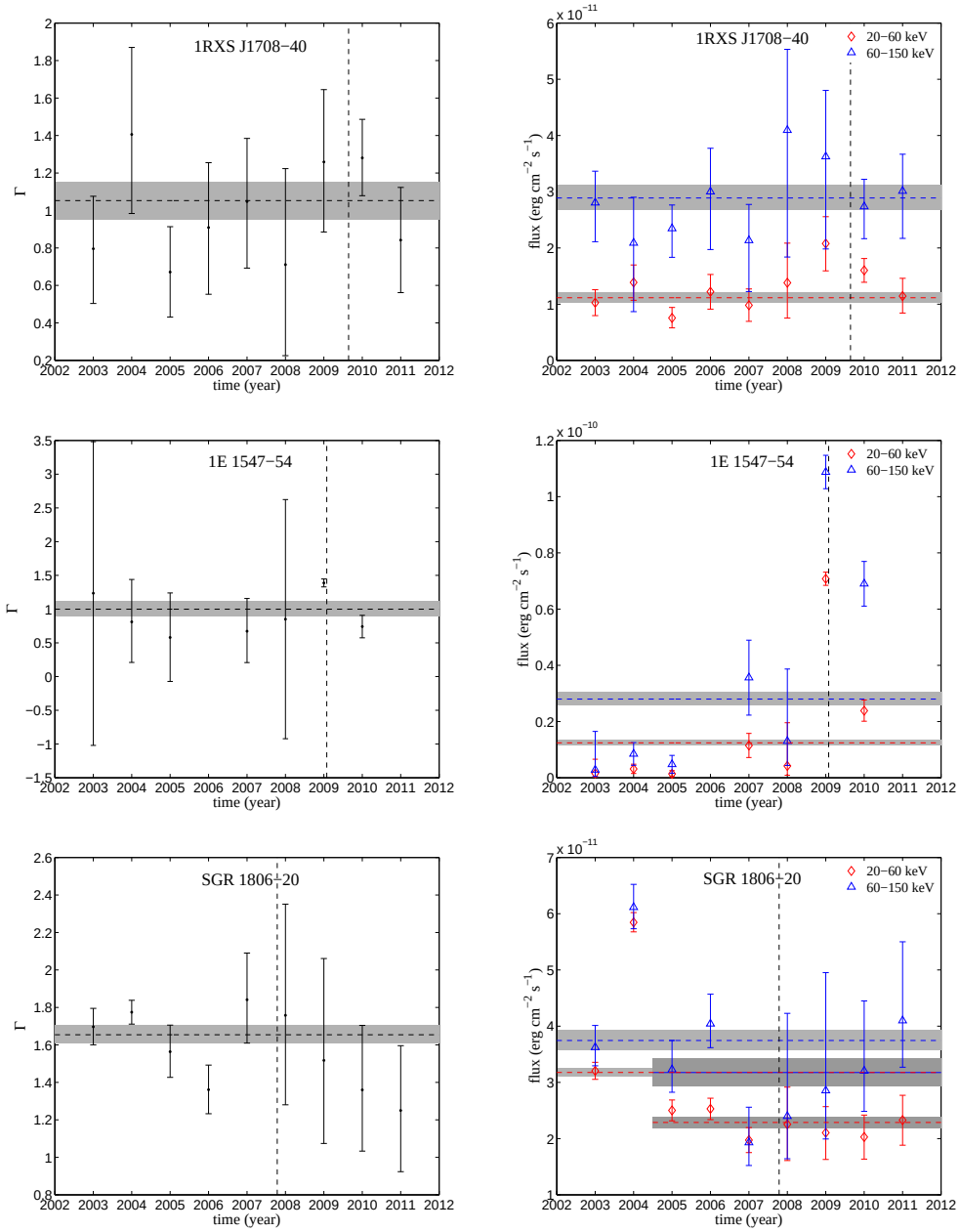

Fig. 1 Photon indices (*left panels*) and fluxes (*right panels*) for every one-year time interval of 1RXS J1708–40, 1E 1547–54 and SGR 1806–20. Horizontal dashed lines represent time-averaged values, with their 1σ errors indicated by grey bands, and vertical dashed lines indicate the observation time of *Suzaku*. Fluxes in the energy range of 20–60 keV and 60–150 keV are in red (*with diamond symbols*) and in blue (*with triangle symbols*) respectively. For SGR 1806–20, time-averaged values from 2005 to 2011 are also plotted.

Table 4 Fitting Results of *Suzaku* Data with the compTB Model

	1RXS J1708–40	1E 1547–54	SGR 1806–20	SGR 0501+45
$N_{\rm H}(10^{22}{\rm cm}^{-2})$	1.50 ± 0.01	3.42 ± 0.03	$7.80^{+0.15}_{-0.14}$	0.79 ± 0.01
$kT_{\rm s}$ (keV)	1.07 ± 0.01	1.17 ± 0.02	1.06 ± 0.02	1.09 ± 0.01
γ	$0.26^{+0.01}_{-0.17}$	0.79 ± 0.04	0.20 ± 0.01	1.27 ± 0.01
α	0.62 ± 0.01	0.60 ± 0.01	0.32 ± 0.01	$0.28^{+0.04}_{-0.03}$
δ	$44.0^{+15.4}_{-7.0}$	$1.34^{+3.04}_{-1.21}$	$200(> 9.23)$	$18.6^{+2.8}_{-1.9}$
$kT_{\rm e}$ (keV)	1.57 ± 0.06	$31.1^{+5.0}_{-4.6}$	$34.2^{+7.2}_{-5.8}$	$3.29^{+0.46}_{-0.31}$
log(A)	-0.58 ± 0.01	-0.47 ± 0.01	-1.44 ± 0.02	-1.25 ± 0.02
$\chi^2_{\rm r}$ (d.o.f.)	1.108 (177)	1.003 (102)	1.008 (95)	1.13 (237)

Table 5 Fitting Results of *Suzaku* and INTEGRAL Data with the compTB Model

	1RXS J1708–40	1E 1547–54	SGR 1806–20
$N_{\rm H}(10^{22}{\rm cm}^{-2})$	1.52 ± 0.01	3.40 ± 0.03	7.89 ± 0.15
$kT_{\rm s}$ (keV)	1.16 ± 0.01	1.14 ± 0.03	0.89 ± 0.02
γ	0.12 ± 0.01	0.82 ± 0.02	0.17 ± 0.01
α	0.43 ± 0.01	0.72 ± 0.02	0.67 ± 0.01
δ	50.8 ± 1.7	$36.5^{+29.6}_{-5.6}$	$31.8^{+2.4}_{-2.0}$
$kT_{\rm e}$ (keV)	2.11 ± 0.06	$3.78^{+0.81}_{-0.48}$	$3.48^{+0.22}_{-0.18}$
log(A)	-1.54 ± 0.01	-0.18 ± 0.02	-0.43 ± 0.03
χ^2_r (d.o.f.)	1.14 (173)	1.01 (94)	0.92 (86)

the spectral fitting could give different results with similar χ^2. We list some fitting results in Table 4, and the corresponding spectra are shown in Figure 2. The parameters are poorly constrained, with the problem mainly lying in the degeneracy of δ and $kT_{\rm e}$. δ ranges from $\sim$1 to $\sim$100 and $kT_{\rm e}$ ranges from $\sim$1 keV to $\sim$10 keV. This should be attributed to the low S/N of *Suzaku* data in the hard X-ray band, but the equivalence of the BMC and TC processes in upscattering seed photons might cause such a situation to some extent.

The parameter γ is left free in spectral fitting, and its best-fit values are in the range of 0.18–1.2, indicating a significant modification to the seed spectrum. Such large deviation of the seed spectrum from a pure blackbody is questionable, so we freeze γ at 3 and try to fit the spectra with compTB again. The spectra of 1E 1547–54 and SGR 1806–20 can be fitted with a larger χ^2, and $kT_{\rm s}$ is similar to the temperature of a blackbody plus a power-law fit to soft X-ray data. However, 1RXS J1708–40 and SGR 0501+45 cannot get acceptable fits. On the other hand, the broadband spectra of 1E 1547–54 and SGR 1806–20 could be fitted with an absorbed blackbody plus power-law model, but an additional blackbody component is required for the spectral fitting of 1RXS J1708–40 and SGR 0501+45.

To better constrain the parameters, we replace the hard X-ray spectra with ISGRI data, which are detected up $\sim$150 keV, higher than the $\sim$70 keV limit of HXD. The compTB model could also be used to produce a good fit to the joint *Suzaku* XIS and IBIS-ISGRI spectra, though giving a slightly worse reduced χ^2 than the former results of *Suzaku* data. The degeneracy of δ and $kT_{\rm e}$ is partly removed, and a set of parameters with apparently better reduced χ^2 can be found. The best fit parameters are shown in Table 5, and the corresponding unfolded spectra are presented in Figure 3. The fitting results of δ and $kT_{\rm e}$ for the three sources do not differ much from each other. The electron temperature $kT_{\rm e}$ is in the range of 2.11–3.48 keV, a little higher than the blackbody temperature $kT_{\rm s}$. However, the values of δ vary from 31.8 to 51.8, showing that the BMC process would be dominant over the TC process.

We also draw error contours for different values of δ and $kT_{\rm e}$ to explore the reliability of fitting results, as shown in Figure 4. For 1RXS J1708–40, there is a satisfying constraint for the two parameters; but the parameters of 1E 1547–54 are not well constrained, as a result of the relatively short

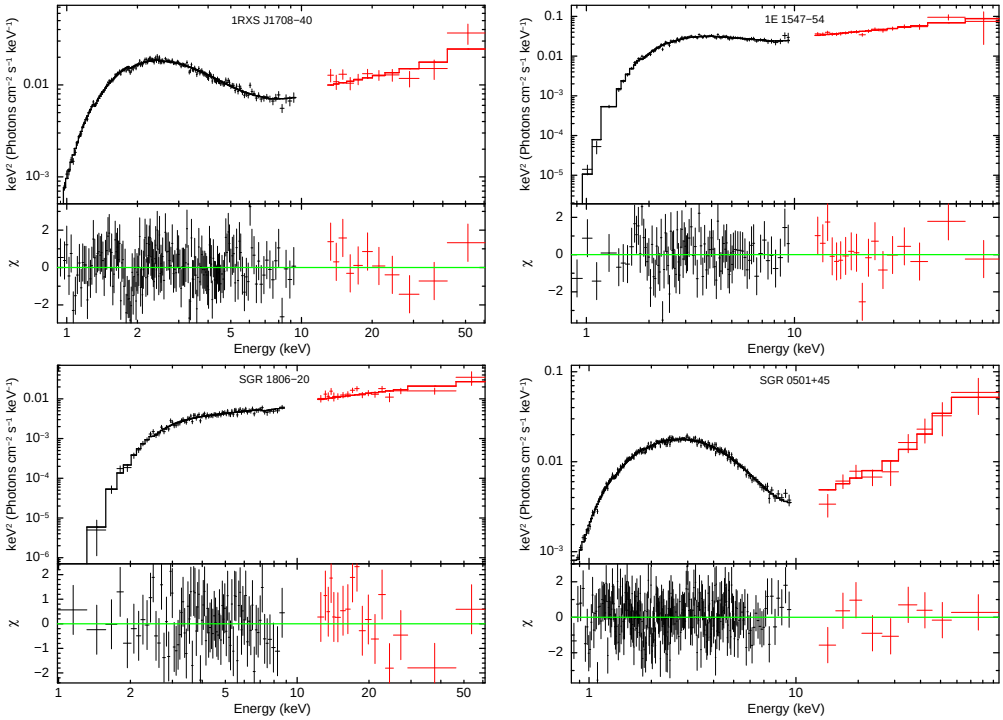

Fig. 2 $E^2 f(E)$ spectra of the four studied AXPs/SGRs, along with the best-fit compTB models and residuals in units of σ. *Suzaku* XIS and HXD data are in black and red respectively.

exposure time of the INTEGRAL data utilized; the situation of SGR 1806–20 is similar to that of 1RXS J1708–40.

4 HXMT SIMULATION

Although IBIS-ISGRI covers the 20–500 keV energy band, data points above ∼150 keV have low S/N, and the spectra are insufficient to differentiate models. The first space telescope developed by China, HXMT, will be launched in late 2014 or early 2015. HXMT will be a collimated hard X-ray telescope based on the direct demodulation method and NaI(Tl)/CsI(Na) phoswich detecting techniques. The payload consists of three telescopes; they work in the low, middle and high energy range respectively, covering the 1–250 keV energy band. Among them, the high energy telescope, sensitive between 20 and 250 keV, has a large collecting area of 5000 cm^2 and hence high sensitivity. Based on the fitting results of the compTB model in Table 5, we simulate spectra with the HXMT response matrix and background file, shown by green lines in Figure 5. With an exposure time of 1 Ms, obvious cutoff around 200 keV can be seen for the three sources.

The simulated spectra are also fitted with the compTB model to examine the improvement in parameter constraints, and the fitting results are listed in Table 6. The errors associated with δ and $kT_{\rm e}$ are much smaller than the results of *Suzaku* and INTEGRAL data, but the constraints on other parameters are similar. Error contours of δ and $kT_{\rm e}$ are also drawn in Figure 6, which exhibit better constraints than those in Figure 4.

In the frame of magnetars, the hard X-ray spectrum is generally expected to be power-law with different cutoff properties. The model based on quantum electrodynamics by Heyl & Hernquist

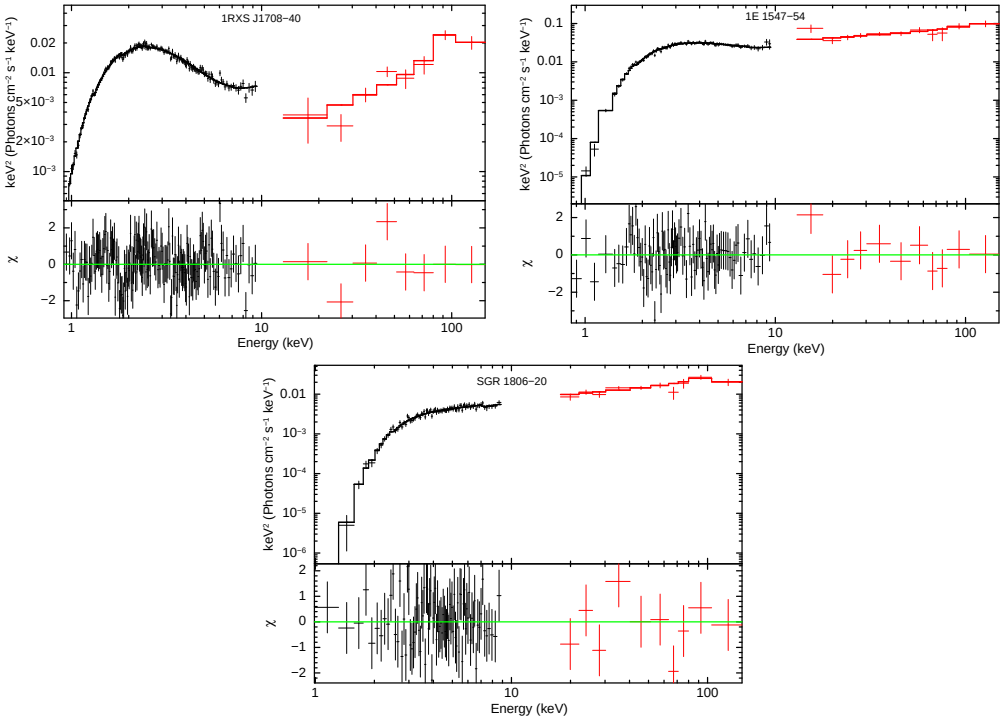

Fig. 3 $E^2 f(E)$ spectra of the three studied AXPs/SGRs, along with the best-fit compTB models and residuals in units of σ. *Suzaku* XIS and INTEGRAL IBIS-ISGRI data are in black and red respectively.

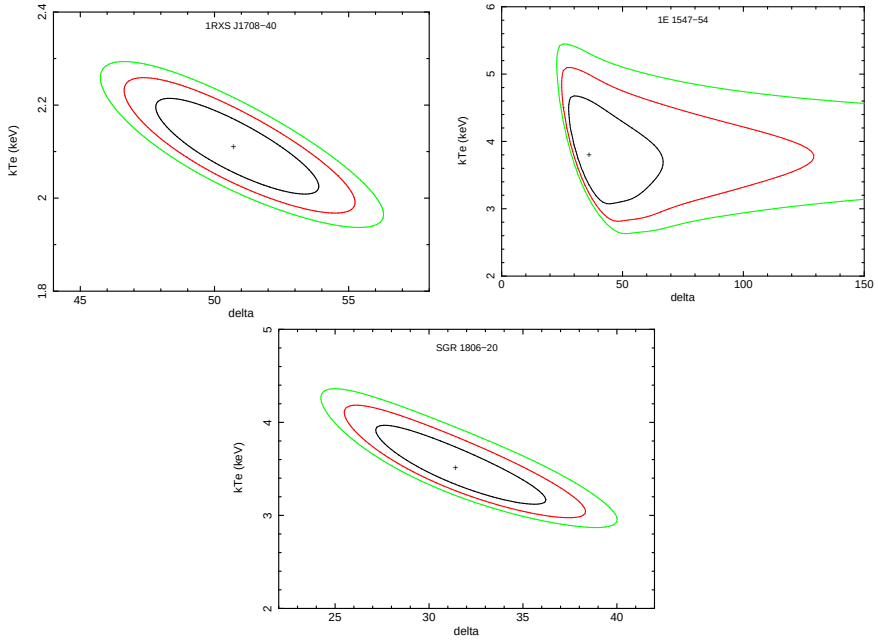

Fig. 4 Error contours of δ(delta) and $kT_{\rm e}$, for compTB fitting to *Suzaku* and INTEGRAL data of 1RXS J1708–40, 1E 1547–54 and SGR 1806–20. The sign '+' indicates parameter values with the minimum χ^2. 1σ, 2σ and 3σ contours are in black, red and green respectively.

Table 6 Fitting Results of Simulated HXMT Data with the compTB Model

	1RXS J1708–40	1E 1547–54	SGR 1806–20
$N_{\rm H}(10^{22}{\rm cm}^{-2})$	1.51 ± 0.01	3.33 ± 0.01	$8.60^{+0.35}_{-0.33}$
$kT_{\rm s}$ (keV)	$1.17^{+0.05}_{-0.01}$	1.11 ± 0.01	0.86 ± 0.03
γ	0.13 ± 0.01	0.94 ± 0.01	0.21 ± 0.02
α	0.43 ± 0.01	0.72 ± 0.01	0.68 ± 0.01
δ	45.4 ± 0.2	32.0 ± 0.4	36.9 ± 0.7
$kT_{\rm e}$ (keV)	2.32 ± 0.01	4.25 ± 0.05	$2.97^{+0.06}_{-0.05}$
log(A)	-1.53 ± 0.01	-0.27 ± 0.01	$-0.31^{+0.06}_{-0.05}$
χ^2_r (d.o.f.)	0.95 (220)	1.15 (337)	1.03 (146)

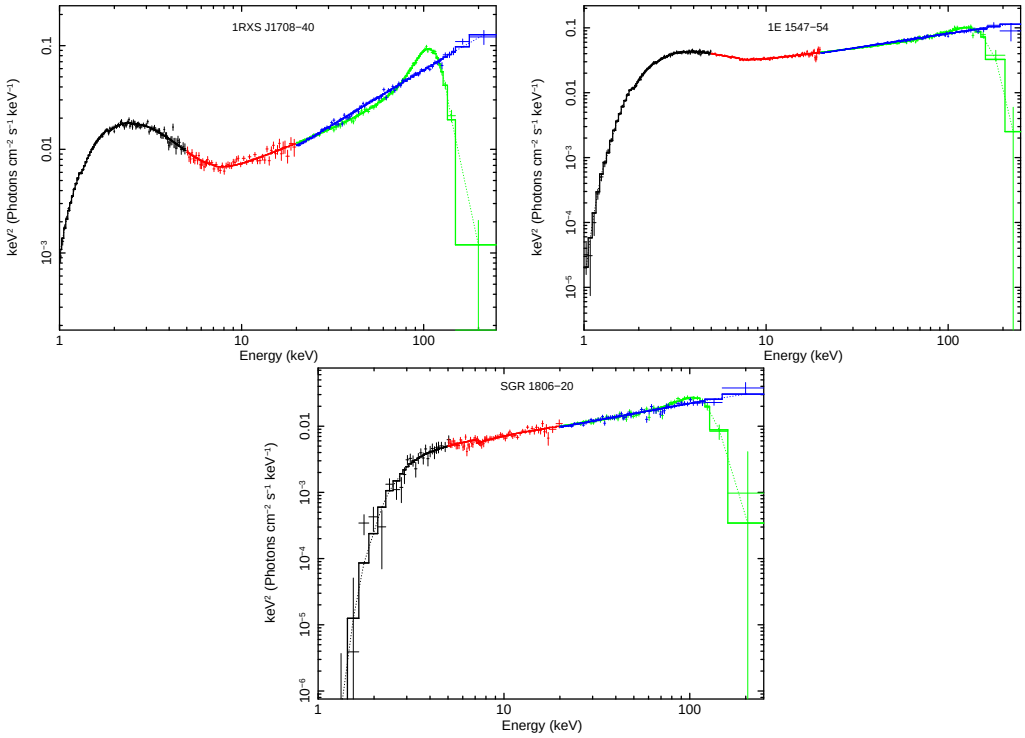

Fig. 5 HXMT simulated spectra of 1RXS J1708–40, 1E 1547–54 and SGR 1806–20. The low (*in black*) and middle (*in red*) energy bands are based on the parameters of the compTB model, but the high energy spectra are simulated for both the compTB and power-law model, shown in green and blue respectively.

(2005) predicts a cutoff energy far above 1 MeV and high flux in the γ-ray band. However, the γ-ray flux of 4U 0142+61 is not detected by Fermi-LAT (Şaşmaz Muş & Göğüş 2010). The bremsstrahlung model by Beloborodov & Thompson (2007) might have a cutoff at a few hundred keV, but the emerging spectrum below the break energy will have a photon index of $\Gamma \sim 1$ for all sources, which is inconsistent with current observations. The resonant inverse Compton scattering model (Baring & Harding 2007) also predicts a power-law with cutoff energy higher than 1 MeV. These hard X-ray models within the frame of magnetars can thus be represented by a power-law without a cutoff below 250 keV.

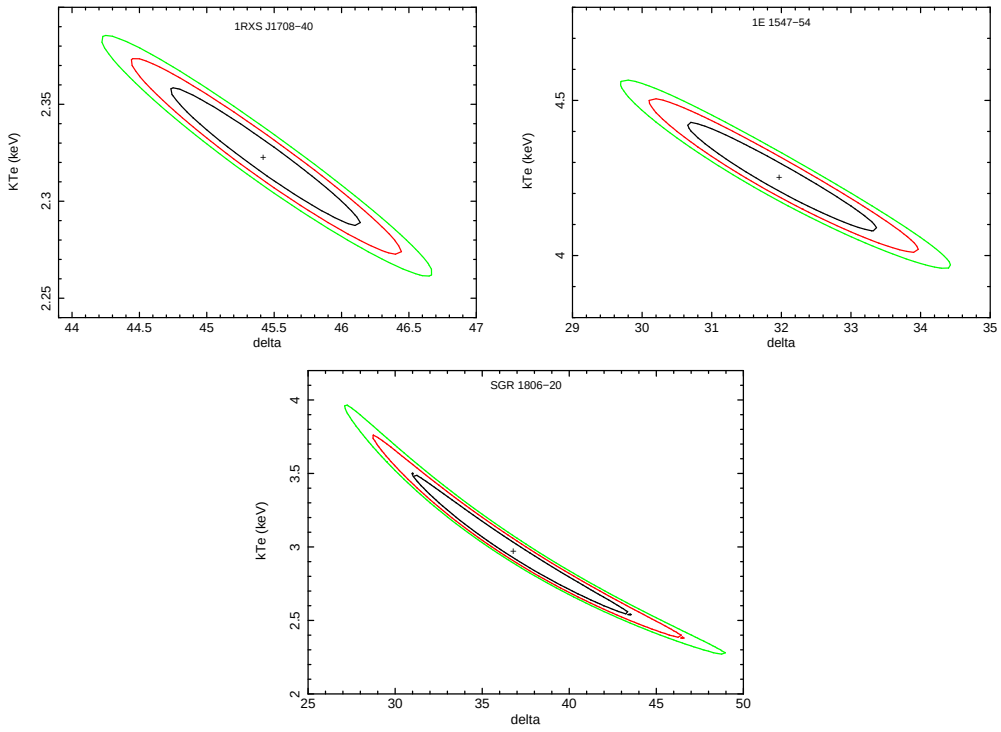

Fig. 6 Error contours of δ(delta) and $kT_{\rm e}$ for compTB fitting to HXMT simulated spectra of 1RXS J1708–40, 1E 1547–54 and SGR 1806–20. The sign '+' indicates parameter values with the minimum χ^2. 1σ, 2σ and 3σ contours are in black, red and green respectively.

According to the parameters of power-law fitting to the ISGRI data in Table 3, we also simulate the HXMT spectra of the power-law model, shown by the blue lines in Figure 5. Comparing the HXMT simulations of the power-law and BMC model, there are obvious discrepancies above $\sim$100 keV, since the spectra of the BMC model could have a cutoff around 200 keV; below $\sim$100 keV, spectra of the two models are roughly similar, but there are also differences in the details. The relatively low cutoff energy of the BMC model results from the low electron temperature, different from ultrarelativistic electrons in other models. The quality of INTEGRAL spectra is not able to discriminate these differences, but future HXMT observations should have spectral resolution and S/N high enough to distinguish between those models. In addition, as we still lack observational data in the 10–20 keV range, the complete 1–250 keV HXMT spectra could provide more information and put better constraints on theoretical models.

5 CONCLUSIONS

Whether AXPs/SGRs are magnetars or quark star/fallback disk systems remains a problem that needs to be settled. We study the soft and hard X-ray spectra of four AXPs/SGRs with *Suzaku* and INTEGRAL observations. The broadband *Suzaku* spectra could be well reproduced by the BMC process, and the BMC model could also fit the combined *Suzaku* and INTEGRAL spectra, with parameters better constrained. Thus the fallback disk system could be compatible with the X-ray emission of AXPs/SGRs, implying that the existence of accretion flow is possible. In addition, HXMT simulated spectra of the BMC model exhibit cutoff around 200 keV, showing a significant discrepancy

from the power-law spectra. We can expect to be able to distinguish the BMC model from other hard X-ray models in research related to magnetars using future observations from the Chinese satellite HXMT, which will allow astronomers to further understand the nature of AXPs/SGRs.

Acknowledgements We would like to thank useful discussions with the pulsar group at PKU. This research has made use of data and software obtained from NASA's High Energy Astrophysics Science Archive Research Center (HEASARC), a service of the Goddard Space Flight Center and the Smithsonian Astrophysical Observatory. This work is supported by the National Basic Research Program of China (973 program, 2012CB821800), the National Natural Science Foundation of China (Grant Nos. 11103019, 11103021, 11225314 and 11203018), the National Fund for Fostering Talents of Basic Science and the XTP project XDA04060604.

References

Alcock, C., Farhi, E., & Olinto, A. 1986, ApJ, 310, 261
Alpar, M. A. 2001, ApJ, 554, 1245
Baring, M. G., & Harding, A. K. 2007, Ap&SS, 308, 109
Beloborodov, A. M., & Thompson, C. 2007, ApJ, 657, 967
Bernardini, F., Israel, G. L., Stella, L., et al. 2011, A&A, 529, A19
Şaşmaz Muş, S., & Göğüş, E. 2010, ApJ, 723, 100
Chatterjee, P., Hernquist, L., & Narayan, R. 2000, ApJ, 534, 373
Duncan, R. C., & Thompson, C. 1992, ApJ, 392, L9
Enoto, T., Nakazawa, K., Makishima, K., et al. 2010a, ApJ, 722, L162
Enoto, T., Nakazawa, K., Makishima, K., et al. 2010b, PASJ, 62, 475
Enoto, T., Rea, N., Nakagawa, Y. E., et al. 2010c, ApJ, 715, 665
Esposito, P., Mereghetti, S., Tiengo, A., et al. 2007, A&A, 476, 321
Farinelli, R., Titarchuk, L., Paizis, A., & Frontera, F. 2008, ApJ, 680, 602
Heyl, J. S., & Hernquist, L. 2005, MNRAS, 362, 777
Hurley, K., Boggs, S. E., Smith, D. M., et al. 2005, Nature, 434, 1098
Koyama, K., Tsunemi, H., Dotani, T., et al. 2007, PASJ, 59, 23
Kuiper, L., Hermsen, W., den Hartog, P. R., & Collmar, W. 2006, ApJ, 645, 556
Lebrun, F., Leray, J. P., Lavocat, P., et al. 2003, A&A, 411, L141
Mereghetti, S. 2008, A&A Rev., 15, 225
Rea, N., Israel, G. L., Oosterbroek, T., et al. 2007, Ap&SS, 308, 505
Takahashi, T., Abe, K., Endo, M., et al. 2007, PASJ, 59, 35
Thompson, C., Lyutikov, M., & Kulkarni, S. R. 2002, ApJ, 574, 332
Tong, H., & Xu, R.-X. 2011, International Journal of Modern Physics E, 20, 15
Tong, H., Xu, R. X., Song, L. M., & Qiao, G. J. 2013, ApJ, 768, 144
Trümper, J. E., Zezas, A., Ertan, Ü., & Kylafis, N. D. 2010, A&A, 518, A46
Ubertini, P., Lebrun, F., Di Cocco, G., et al. 2003, A&A, 411, L131
Wang, W., Tong, H., & Guo, Y.-J. 2013, arXiv:1311.0107
Winkler, C., Courvoisier, T. J.-L., Di Cocco, G., et al. 2003, A&A, 411, L1
Xu, R. X. 2003, ApJ, 596, L59
Xu, R. 2007, Advances in Space Research, 40, 1453
Xu, R. X., Tao, D. J., & Yang, Y. 2006, MNRAS, 373, L85